

## Molecularly Defined Caprolactone Oligomers and Polymers: Synthesis and Characterization

Kenichi Takizawa,<sup>†,‡</sup> Chuanbing Tang,<sup>†</sup> and Craig J. Hawker<sup>\*†</sup>

Materials Research Laboratory and Departments of Materials, Chemistry and Biochemistry, University of California, Santa Barbara, California 93106, and Mitsubishi Chemical Group Science and Technology Research Center, Inc., 1000 Kamoshida-cho, Aoba-ku, Yokohama, 227-8502, Japan

Received September 14, 2007; E-mail: hawker@mrl.ucsb.edu

**Abstract:** The synthesis of molecularly defined  $\epsilon$ -caprolactone oligomers and polymers up to the 64-mer, via an exponential growth strategy, is described. By careful selection of orthogonal protecting groups, *t*-butyldimethylsilyl (TBDMS) ether for the hydroxyl group and benzyl (Bn) ester for the carboxylic acid group, a highly efficient synthetic strategy was developed with yields for both deprotection steps being essentially quantitative and for the coupling reactions using 1,3-dicyclohexylcarbodiimide (DCC), yields of 80–95% were obtained even at high molecular weights. This allows monodisperse dimers, tetramers, octamers, 16-mers, 32-mers and 64-mers to be prepared in gram quantities and fully characterized using mass spectroscopy, size exclusion chromatography (SEC), and IR and NMR spectroscopy. Thermal and physical properties were measured using thermogravimetric analysis (TGA), differential scanning calorimetry (DSC), atomic force microscopy (AFM), and small-angle X-ray scattering (SAXS). These results conclusively show a distinct structure/property relationship with a close correlation between the number of repeat units and physical properties. In addition, a number of marked differences were observed on comparison with the parent poly(caprolactone) polymer.

### Introduction

A wide range of biocompatible, biodegradable, and resorbable synthetic polymers has been developed for bioengineering and biomedical applications with poly(caprolactone) (PCL) being one of the most widely studied synthetic materials.<sup>1</sup> The leading role of PCL as a biomaterial is further evidenced by its approval by the Food and Drug Administration (FDA) for use in the human body as a drug delivery device, suture (sold under the brand name Monocryl), adhesion barrier, and is being investigated as a scaffold for tissue engineering. Over time, the ester groups in the backbone of PCL undergo hydrolysis to the constituent hydroxy acid which is eliminated by general metabolic pathways.<sup>2</sup> Unfortunately, most implanted materials are seen by the body as foreign objects, which leads to a range of undesirable immune responses. The recent negative publicity regarding drug-covered stents is a perfect example of the significant unmet medical need for both the rational design of functionalized synthetic biomaterials as well as a complete understanding of structure/property relationships.

Traditionally, poly(caprolactone) has been prepared via the ring opening polymerization of  $\epsilon$ -caprolactone using a catalyst such as stannous octanoate with significant effort in recent years being devoted to living processes,<sup>3</sup> complex macromolecular architectures,<sup>4</sup> and metal-free systems.<sup>5</sup> The resulting polymer is semicrystalline with a  $T_m$  of 58–60 °C and is widely used as a reactive block in the preparation of copolymers as well as in blends with other commodity polymers. Although there is a growing academic and industrial interest in poly(caprolactone)

<sup>†</sup> University of California.

<sup>‡</sup> Mitsubishi.

(1) (a) Ha, C.-S.; Gardella, J. A., Jr. *Chem. Rev.* **2005**, *105*, 4205–4232. (b) Grayson, S. M.; Frechet, J. M. J. *Chem. Rev.* **2001**, *101*, 3819–3868. (c) Altheld, A.; Feng, Y.; Kelch, S.; Lendlein, A. *Angew. Chem., Int. Ed.* **2005**, *44*, 1188–1192. (d) Kopecek, K.; Ulbrich, K. *Prog. Polym. Sci.* **1993**, *9*, 1.  
(2) (a) Echeverria, E.; Jimenez, J. *Surgery* **1970**, *131*, 1. (b) Alexander, H.; Parsons, J. R.; Straucher, I. D.; Corcoran, S. F.; Gona, O.; Mayott, C.; Weiss, A. B. *Orthop. Rev.* **1981**, *10*, 41. (c) Sawhney, A. S.; Pathak, C. P.; Hubbell, J. A. *Macromolecules* **1993**, *26*, 581.

(3) (a) Wisse, E.; Renken, R. A. E.; Roosma, J. R.; Palmans, A. R. A.; Meijer, E. W. *Biomacromolecules* **2007**, *8*, 2739–2745. (b) Parrish, B.; Breitenkamp, R. B.; Emrick, T. *J. Am. Chem. Soc.* **2005**, *127*, 7404–7410. (c) O'Keefe, B. J.; Breyfogle, L. E.; Hillmyer, M. A.; Tolman, W. B. *J. Am. Chem. Soc.* **2002**, *124*, 4384–4393. (d) Trollsas, M.; Atthoff, B.; Claesson, H.; Hedrick, J. L. *J. Polym. Sci., Part A: Polym. Chem.* **2004**, *42*, 1174–1188. (e) Hedrick, J. L.; Magbitang, T.; Connor, E. F.; Glauser, T.; Volksen, W.; Hawker, C. J.; Lee, V. Y.; Miller, R. D. *Chem.-Eur. J.* **2002**, *8*, 3308–3319. (f) Ovit, T. M.; Coates, G. W. *J. Am. Chem. Soc.* **2002**, *124*, 1316–1326. (g) Van, Horn, B. A.; Wooley, K. L. *Soft Matter* **2007**, *3*, 1032–1040.  
(4) (a) Barrera, D. A.; Zylstra, E.; Lansbury, P. T.; Langer, R. J. *J. Am. Chem. Soc.* **1993**, *115*, 11010. (b) Tian, D.; Dubois, Ph.; Grandfils, C.; Jérôme, J. *Macromolecules* **1997**, *30*, 406. (c) Trollsas, M.; Lee, V. Y.; Mecerreyes, D.; Löwenhielm, P.; Möller, M.; Miller, R. D.; Hedrick, J. L. *Macromolecules* **2000**, *33*, 4619. (d) Lenoir, S.; Riva, R.; Detrembleur, C.; Jérôme, R.; Lecomte, P. *Macromolecules* **2004**, *37*, 4055. (e) Zhang, Q.; Remsen, E. E.; Wooley, K. L. *J. Am. Chem. Soc.* **2000**, *122*, 3642–3651. (f) Moller, M.; Nederberg, F.; Lim, L. S.; Kange, R.; Hawker, C. J.; Hedrick, J. L.; Gu, Y. D.; Shah, R.; Abbott, N. L. *J. Polym. Sci., Part A: Polym. Chem.* **2001**, *39*, 3529–3538.  
(5) (a) Coulembier, O.; Kiesewetter, M. K.; Mason, A.; Dubois, P.; Hedrick, J. L.; Waymouth, R. M. *Angew. Chem., Int. Ed. Engl.* **2007**, *46*, 4719–4721. (b) Coulembier, O.; Degee, P.; Hedrick, J. L. *Prog. Polym. Sci.* **2006**, *31*, 723–747. (c) Cordova, A.; Hult, A.; Hult, K.; Ihre, H.; Iversen, T.; Malmstrom, E. *J. Am. Chem. Soc.* **1998**, *120*, 13521–13522. (d) Chen, B.; Miller, M. E.; Gross, R. A. *Langmuir* **2007**, *23*, 6467–6474. (e) Marcilla, R.; de Geus, M.; Mecerreyes, D.; Duxbury, C. J.; Koning, C. E.; Heise, A. *Eur. Polym. J.* **2006**, *42*, 1215–1221.

and biodegradable polyesters in general, there have been no studies on the synthesis of well-defined oligomers based on poly(caprolactone), poly(lactide), etc. This is unfortunate because the availability of precisely defined oligomers<sup>6</sup> would enable a wide range of structure property studies to fully understand, predict, and tune the degradation rate, crystal structure, self-assembly, and performance of these materials in a variety of applications.

The significant benefit afforded material design by the development of synthetic approaches to well-defined oligomers arises from a fundamental understanding of the parent polymer through the availability and detailed study of dimers, tetramers, octamers, etc. Previous work has demonstrated the power of this approach with molecular-defined oligomers being produced in both cellular systems<sup>7</sup> as well as in stepwise synthetic strategies.<sup>8</sup> Of particular note is the work of Brooke,<sup>8b,c</sup> who has prepared a series of oligomers related to commercially important polymers such as Nylon 6,6 and poly(ethylene terephthalate). In addition, Moore<sup>9</sup> has demonstrated the change in conformation and associated physical/chemical properties of poly(phenyleneethynyls) with oligomer length. Similarly, Meijer<sup>10</sup> has shown that well-defined  $\pi$ -conjugated oligomers, such as sexithiophene can play an important role in the field of organic electronics due to their precise chemical structure and conjugation length which gives rise to well-defined electronic properties and tunable intermolecular solid state organization. These and other studies demonstrating the syntheses of molecular rods of precise length<sup>11</sup> have illustrated the dramatic insights that can be gained from the study of well-defined oligomers and polymeric derivatives of both scientifically and industrially important macromolecules. Herein, we report the development of a synthetic strategy for the synthesis of well-defined polyester oligomers and demonstrate the preparation of a series of poly-(caprolactone) derivatives up to the 64-mer. The physical and structural properties of these essentially single molecule species allow a fundamental insight into the physical and structural properties of the widely studied parent polymer.

## Experimental Section

**Materials and General Procedures.** 4-(Dimethylamino)pyridinium *p*-toluenesulfonate (DPTS) was synthesized according to a previously reported procedure.<sup>12</sup> All of the other chemicals and solvents were purchased from Aldrich, of reagent grade, and used without further purification. Analytical TLC was performed on commercial Merck Plates coated with silica gel GF254 (0.24 mm thick). Silica gel for flash column chromatography was Merck Kieselgel 60 (230–400 mesh, ASTM). <sup>1</sup>H NMR (200 MHz) and <sup>13</sup>C NMR (100 MHz) measurements were performed on a Bruker AC 200 spectrometer at room temperature.

- (6) (a) Zhang, J.; Moore, J. S.; Xu, Z.; Aguirre, R. A. *J. Am. Chem. Soc.* **1992**, *114*, 2273. (b) Zhou, X. Z.; Shea, K. J. *J. Am. Chem. Soc.* **2000**, *122*, 11515–11516.
- (7) Krejchi, M. T.; Atkins, E. D. T.; Waddon, A. J.; Fournier, M. J.; Mason, T. L.; Tirrell, D. A. *Science* **1994**, *265*, 1427–1432.
- (8) (a) Hawker, C. J.; Malmstrom, E. E.; Frank, C. W.; Kampf, J. P. *J. Am. Chem. Soc.* **1997**, *119*, 9903. (b) Brooke, G. M.; MacBride, J. A. H.; Mohammed, S.; Whiting, M. C. *Polymer* **2000**, *41*, 6457. (c) Brooke, G. M.; Cameron, N. R.; MacBride, J. A. H.; Whiting, M. C. *Polymer* **2002**, *43*, 1139.
- (9) Stone, M. T.; Heemstra, J. M.; Moore, J. S. *Acc. Chem. Res.* **2006**, *39*, 11–20.
- (10) Leclere, P.; Surin, M.; Viville, P.; Lazzaroni, R.; Kilbinger, A. F. M.; Henze, O.; Feast, W. J.; Cavallini, M.; Biscarini, F.; Schenning, A. P. H. J.; Meijer, E. W. *Chem. Mater.* **2004**, *16*, 4452–4466.
- (11) Gothard, C. M.; Rao, N. A.; Nowick, J. S. *J. Am. Chem. Soc.* **2007**, *129*, 7272–7273.
- (12) (a) Moore, J. S.; Stupp, S. I. *Macromolecules* **1990**, *23*, 65. (b) Hawker, C. J.; Fréchet, J. M. J. *J. Chem. Soc., Perkin Trans 1* **1992**, 2459–2469.

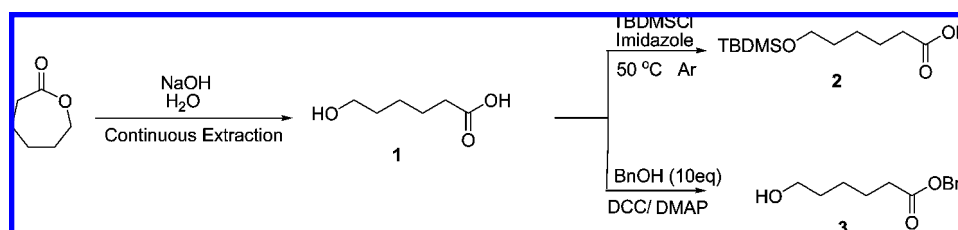
Matrix assisted laser desorption/ionization (MALDI-TOF-MS) was carried out at room temperature on a Dynamo Thermo machine using dithranol in THF as the matrix and sodium trifluoroacetate (NaOTf) in THF as the cation agent. Size exclusion chromatography (SEC) was carried out at room temperature on a Waters Alliance HPLC System (Waters 2695 Separation Module) connected to Waters Styragel HR columns (HR 0.5, 2, and 4) using THF as eluent (flow rate: 1 mL/min). A Waters 2414 differential refractometer and a 2996 photodiode array detector were employed. Preparative GPC was carried out at room temperature on a Waters 1525 Binary HPLC connected to a Waters 2414 differential refractometer and Waters Styragel columns (Ultrastryragel 100, 10<sup>-3</sup>, and 10<sup>-4</sup> Å) using THF as eluent (flow rate: 6 mL/min). The molecular weights of the polymers were calculated relative to linear polystyrene standards. Thermogravimetric analysis was conducted using Mettler TGA/DTA 851e under N<sub>2</sub> atmosphere. Differential scanning calorimetry (DSC) measurements were performed with a TA Instruments DCS 2920 and a ramp rate of 5 degrees per minute with data collected during third cycle in the selected temperature ranges. Calibrations were made using indium as a standard for both temperature transitions and the heats of fusion. Melting transition temperatures (*T*<sub>m</sub>) were determined as the peak maxima of the transition. Small-angle X-ray scattering (Ultra-SAXS (X-ray Source; Fine focus (0.2 mm) Rigaku rotating anode generator, Wavelength; 1.54 Å, Sample to Detector Distance; 172.5 cm, Interface; Bruker SAXS software and SPEC) and Intermediate-SAXS (X-ray Source; 18kW Rigaku rotating anode generator, Wavelength; 1.54 Å, Sample to Detector Distance; 75.8 cm, Interface; SPEC)) were carried out using quartz capillary cell. Tapping mode AFM experiments were carried out using a Multimode Nanoscope III system equipped with a J-type vertical engage scanner (Digital Instruments, Santa Barbara, CA). The measurements were performed under ambient atmosphere using commercial Si cantilevers with a nominal spring constant and resonance frequency respectively equal to 48 N/m and 190 kHz (ACL, Applied Nanostructures, Santa Clara, CA).

### General Procedure of Coupling Reaction: Synthesis of Dimer

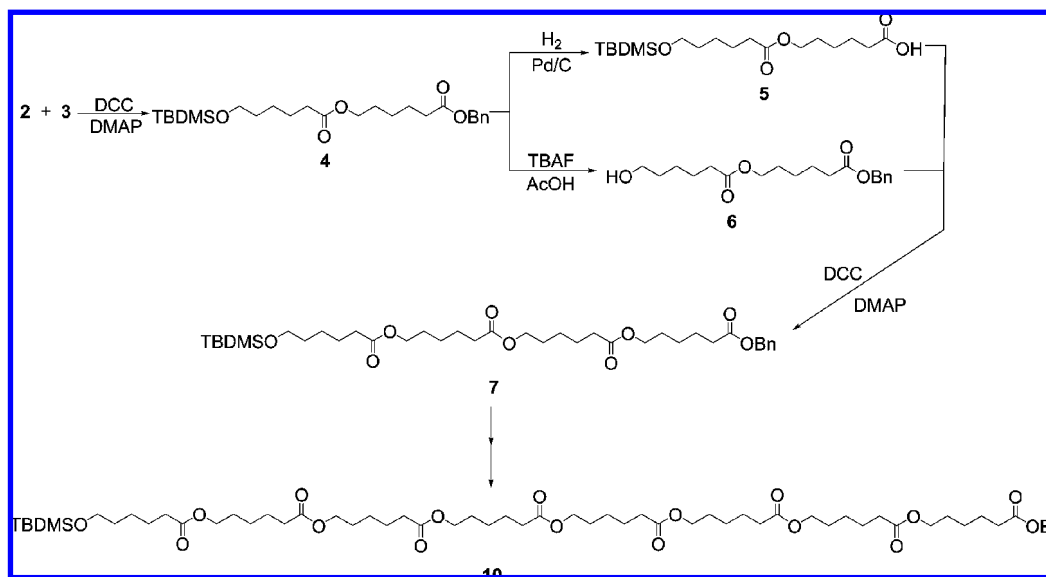
**4.** A mixture of the protected acid **2** (20.50 g, 83.19 mmol), protected alcohol **3** (17.74 g, 79.81 mmol), 1,3-dicyclohexylcarbodiimide (DCC) (19.29 g, 93.49 mmol), and 4-(dimethylamino)pyridine (DMAP) (11.17 g, 91.43 mmol) was dissolved in CH<sub>2</sub>Cl<sub>2</sub> (200 mL) and stirred overnight at room temperature. The resulting mixture was filtered and the filtrate poured into a separatory funnel and washed with 200 mL of sat. CuSO<sub>4</sub> and 200 mL of H<sub>2</sub>O. The organic layer was then dried over MgSO<sub>4</sub>, filtered, and concentrated under reduced pressure. The crude product was purified via flash chromatography using 3:1 hexanes/ethyl acetate as eluent to give the doubly protected dimer, **4**, as a clear, colorless oil (29.60 g, 81% yield); <sup>1</sup>H NMR (CDCl<sub>3</sub>):  $\delta$  7.33 (m, Ar, 5H), 5.10 (s, CO<sub>2</sub>CH<sub>2</sub>Ph, 2H), 4.03 (t, *J* = 6.5 Hz, CO<sub>2</sub>CH<sub>2</sub>CH<sub>2</sub>, 2H), 3.58 (t, *J* = 6.3 Hz, CH<sub>2</sub>OSi, 2H), 2.31 (t, t, *J* = 7.6 Hz, 7.6 Hz, CH<sub>2</sub>CH<sub>2</sub>CO<sub>2</sub>, CH<sub>2</sub>CH<sub>2</sub>CO<sub>2</sub>, 4H), 1.50 (m, SiOCH<sub>2</sub>[CH<sub>2</sub>]<sub>3</sub>CH<sub>2</sub>CO<sub>2</sub>CH<sub>2</sub>[CH<sub>2</sub>]<sub>3</sub>CH<sub>2</sub>CO<sub>2</sub>-CH<sub>2</sub>Ph, 12H), 0.88 (s, (CH<sub>3</sub>)<sub>3</sub>CSi, 9H), 0.04 (s, (CH<sub>3</sub>)<sub>2</sub>Si, 6H). <sup>13</sup>C NMR (CDCl<sub>3</sub>):  $\delta$  173.82 (CO, 1C), 173.35 (CO, 1C), 136.15 (Ar, CH<sub>2</sub>-C, 1C) 128.64 (Ar-*meta*, 2C), 128.29 (Ar-*ortho*, *para*, 3C), 66.22 (CO<sub>2</sub>CH<sub>2</sub>Ph, 1C), 64.10 (CO<sub>2</sub>CH<sub>2</sub>CH<sub>2</sub>, 1C), 63.04 (SiOCH<sub>2</sub>, 1C), 34.40 (CH<sub>2</sub>CH<sub>2</sub>CO<sub>2</sub>, 1C), 34.20 (CH<sub>2</sub>CH<sub>2</sub>CO<sub>2</sub>, 1C), 32.56 (SiOCH<sub>2</sub>CH<sub>2</sub>CH<sub>2</sub>, 1C), 28.43 (CO<sub>2</sub>CH<sub>2</sub>CH<sub>2</sub>CH<sub>2</sub>, 1C), 26.06 ((CH<sub>3</sub>)<sub>3</sub>CSi, 3C), 25.61 (CH<sub>2</sub>CH<sub>2</sub>CH<sub>2</sub>, 1C), 25.55 (CH<sub>2</sub>CH<sub>2</sub>CH<sub>2</sub>, 1C), 24.90 (CH<sub>2</sub>CH<sub>2</sub>CH<sub>2</sub>, 1C), 24.66 (CH<sub>2</sub>CH<sub>2</sub>CH<sub>2</sub>, 1C), 18.43 ((CH<sub>3</sub>)<sub>3</sub>CSi, 1C), -5.18 ((CH<sub>3</sub>)<sub>2</sub>Si, 2C). Mass Spec for C<sub>25</sub>H<sub>42</sub>O<sub>5</sub>Si+Na Calculated: 473.2699; Found (M+Na)<sup>+</sup>: 473.2697.

**General Procedure of Deprotection of Benzyl Ester (Hydrogenation): Synthesis of the Acid-Functionalized Dimer, 5.** Palladium on activated carbon (10 wt %, 0.87 g) was added to a solution of **4** (8.28 g, 18.37 mmol) in ethyl acetate (100 mL), and the reaction mixture was stirred overnight at room temperature under hydrogen. The resulting mixture was filtered through celite, the celite washed with 100 mL of

Scheme 1.



Scheme 2.



hot MeOH, and the combined filtrate was concentrated under reduced pressure. Drying under high vacuum then gave the monodeprotected dimer, **5**, as a clear, colorless oil (yield 13.12 g, 100%);  $^1\text{H NMR}$  ( $\text{CDCl}_3$ ):  $\delta$  4.05 (t,  $J = 6.5$  Hz,  $\text{CO}_2\text{CH}_2\text{CH}_2$ , 2H), 3.59 (t,  $J = 6.3$  Hz,  $\text{CH}_2\text{OSi}$ , 2H), 2.32 (t, t,  $J = 7.2$  Hz, 7.2 Hz,  $\text{CH}_2\text{CH}_2\text{CO}_2$ ,  $\text{CH}_2\text{CH}_2\text{CO}_2$ , 4H), 1.50 (m,  $\text{SiOCH}_2[\text{CH}_2]_3\text{CH}_2\text{CO}_2\text{CH}_2[\text{CH}_2]_3\text{CH}_2\text{CO}_2\text{H}$ , 13H) 0.87 (s,  $(\text{CH}_3)_3\text{CSi}$ , 9H), 0.02 (s,  $(\text{CH}_3)_2\text{Si}$ , 6H).  $^{13}\text{C NMR}$  ( $\text{CDCl}_3$ ):  $\delta$  179.68 ( $\text{CO}_2\text{H}$ , 1C), 174.10 ( $\text{CO}_2\text{CH}_2$ , 1C), 64.21 ( $\text{CO}_2\text{CH}_2\text{CH}_2$ , 1C), 63.20 ( $\text{SiOCH}_2$ , 1C), 34.51 ( $\text{CH}_2\text{CH}_2\text{CO}_2$ , 1C), 34.05 ( $\text{CH}_2\text{CH}_2\text{CO}_2$ , 1C), 32.61 ( $\text{SiOCH}_2\text{CH}_2\text{CH}_2$ , 1C), 28.48 ( $\text{CO}_2\text{CH}_2\text{CH}_2\text{CH}_2$ , 1C), 26.14 ( $(\text{CH}_3)_3\text{CSi}$ , 3C), 25.61 ( $\text{CH}_2\text{CH}_2\text{CH}_2$ , 2C), 24.98 ( $\text{CH}_2\text{CH}_2\text{CH}_2$ , 1C), 24.46 ( $\text{CH}_2\text{CH}_2\text{CH}_2$ , 1C), 18.53 ( $(\text{CH}_3)_3\text{CSi}$ , 1C),  $-5.11$  ( $(\text{CH}_3)_2\text{Si}$ , 2C); HRMS-EI ( $m/z$ ):  $[\text{M}]^+$  calcd for  $\text{C}_{18}\text{H}_{36}\text{O}_5\text{Si}$ , 360.2332; found, 360.2333.

**General Procedure of Deprotection of TBDMS Protected Alcohol (Desilylation): Synthesis of Hydroxyl-Terminated Dimer, 6.** A mixture of glacial acetic acid (4.41 g, 73.41 mmol) and tetrabutylammonium fluoride (TBAF) (66.29 g, 73.41 mmol, 1.0 M solution in THF) was added to a solution of **4** (16.55 g, 36.72 mmol) in THF (75 mL). The reaction mixture was stirred overnight at 50 °C and then poured into a separatory funnel containing 300 mL of  $\text{CH}_2\text{Cl}_2$  and 300 mL of  $\text{H}_2\text{O}$ . The organic layer was then washed with sat.  $\text{NaHCO}_3$  (2  $\times$  200 mL), 5 wt % Citric acid (2  $\times$  200 mL), and  $\text{H}_2\text{O}$  (1  $\times$  200 mL), dried over  $\text{MgSO}_4$ , filtered, and concentrated under reduced pressure. The crude product was purified via flash chromatography using 1:1 hexanes/ethyl acetate as eluent to give **6** as a clear, colorless oil (yield 11.45 g, 93% yield);  $^1\text{H NMR}$  ( $\text{CDCl}_3$ ):  $\delta$  7.34 (s, Ar, 5H), 5.11 (s,  $\text{CO}_2\text{CH}_2\text{Ph}$ , 2H), 4.05 (t,  $J = 6.4$  Hz,  $\text{CO}_2\text{CH}_2\text{CH}_2$ , 2H), 3.60 (t,  $J = 6.4$  Hz,  $\text{CH}_2\text{OH}$ , 2H), 2.99 (b, OH, 1H), 2.33 (t, t,  $J = 7.3$  Hz, 7.3 Hz,  $\text{CH}_2\text{CH}_2\text{CO}_2$ ,  $\text{CH}_2\text{CH}_2\text{CO}_2$ , 4H), 1.50 (m,  $\text{HOCH}_2[\text{CH}_2]_3\text{CH}_2\text{CO}_2\text{CH}_2[\text{CH}_2]_3\text{CH}_2\text{CO}_2\text{CH}_2\text{Ph}$ , 12H).  $^{13}\text{C NMR}$  ( $\text{CDCl}_3$ ):  $\delta$  173.69 (CO, 1C), 173.22 (CO, 1C), 135.86 (Ar,  $\text{CH}_2\text{-C}$ , 1C) 128.38 (Ar-*meta*, 2C), 128.00 (Ar-*ortho*, *para*, 3C), 65.97 ( $\text{CO}_2\text{CH}_2\text{Ph}$ , 1C), 63.94 ( $\text{CO}_2\text{CH}_2\text{CH}_2$ , 1C), 62.05 ( $\text{HOCH}_2$ , 1C), 34.06 ( $\text{CH}_2\text{CH}_2\text{CO}_2$ , 1C), 33.92 ( $\text{CH}_2\text{CH}_2\text{CO}_2$ ,

1C), 32.12 ( $\text{HOCH}_2\text{CH}_2\text{CH}_2$ , 1C), 28.13 ( $\text{CO}_2\text{CH}_2\text{CH}_2\text{CH}_2$ , 1C), 25.33 ( $\text{CH}_2\text{CH}_2\text{CH}_2$ , 1C), 25.18 ( $\text{CH}_2\text{CH}_2\text{CH}_2$ , 1C), 24.56 ( $\text{CH}_2\text{CH}_2\text{CH}_2$ , 1C), 24.37 ( $\text{CH}_2\text{CH}_2\text{CH}_2$ , 1C); HRMS-EI ( $m/z$ ):  $[\text{M}]^+$  calcd for  $\text{C}_{18}\text{H}_{28}\text{O}_5$ , 324.1936; found, 324.1935.

## Results and Discussion

The starting monomer, 6-hydroxycaproic acid, **1**, was obtained in essentially quantitative yield by continuous extraction of the base-catalyzed ring opening of commercially available  $\epsilon$ -caprolactone. In designing the appropriate growth strategy for preparation of well-defined oligomers from **1**, the selection of orthogonal protecting groups for the hydroxyl and carboxylic acid groups was critical. After extensive comparison of various protecting groups pairs under growth and deprotection conditions, the most efficient and selective protecting groups were found to be a *t*-butyldimethylsilyl (TBDMS) ether for the hydroxyl group and a benzyl (Bn) ester for the carboxylic acid. Therefore, the hydroxyl group of **1** was protected with *t*-butyldimethylsilyl (TBDMS) ether,<sup>13,14</sup> yielding **2**, and the carboxylic acid group was protected with a benzyl (Bn) ester, yielding the monohydroxy derivative, **3** (Scheme 1).

Having identified orthogonal protecting groups, the next challenge in this exponential growth strategy was to elucidate a reliable connection strategy that would permit large oligomers to be coupled in essentially quantitative yields without cleavage of the hydroxyl or carboxylic acid protecting groups. Initial studies using acyl halide or active ester derivatives of **2** proved to be unsuccessful with either low yields or minor amounts of deprotection of the TBDMS group being observed. In contrast,

(13) Corey, E. J.; Venkateswarlu, A. *J. Am. Chem. Soc.* **1972**, *94*, 6190.

(14) Smith, A. B., III.; Ott, R. G. *J. Am. Chem. Soc.* **1996**, *118*, 13095.

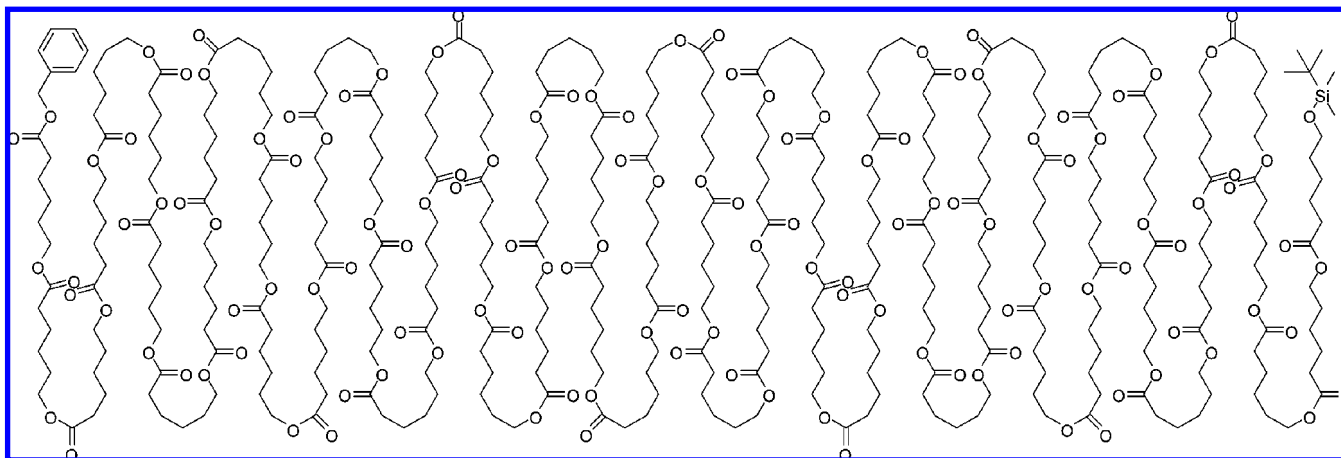


Figure 1. Molecular Structure of  $\epsilon$ -Caprolactone 64-mer, **19**.

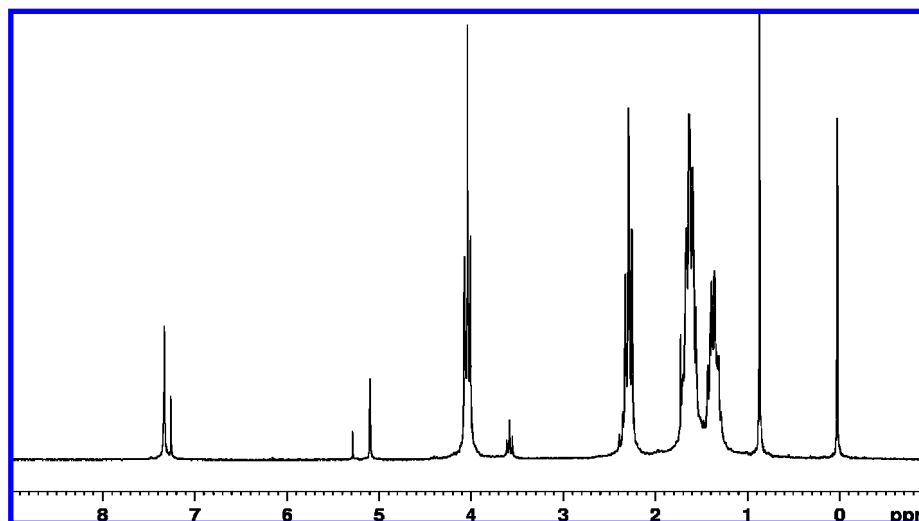


Figure 2.  $^1\text{H}$  NMR spectrum of doubly protected  $\epsilon$ -Caprolactone hexadecamer, **13**.

examination of carbodiimide coupling proved to be successful for low molecular weight oligomers using DCC and DMAP up to the tetramer. For larger oligomers, yields were observed to decrease slightly for the octamer and to decrease significantly for larger molecules. As previously reported,<sup>12</sup> a frequent side reaction of carbodiimide esterifications is the formation of unreactive N-acylureas (DCC-Adducts), which was shown to be the cause of decreasing yields for larger oligomers. Replacement of DMAP with 4-(dimethylamino)pyridinium *p*-toluenesulfonate (DPTS) was found to suppress this side reaction, and even at high molecular weights, only minor amounts (<2%) were observed.

The repetitive chain growth strategy is illustrated in Scheme 2 and involves initial coupling of the carboxylic acid, **2**, with the hydroxyl derivative, **3**, to give the protected dimer, **4**. The tetramer sample is then split and the benzyl group is removed by hydrogenation, affording the desired carboxylic acid, **5**, whereas treatment with tetra-*n*-butyl ammonium fluoride (TBAF) in the presence of acetic acid gives the monohydroxy derivative, **6**. In both cases, the optimized reaction procedures resulted in essentially quantitative yields of the monofunctional dimers. Repetition of this coupling strategy gave the tetramer, **7**, deprotection of which results in the two corresponding monofunctional tetramers, **8** and **9**, and subsequently coupling gives the octamer, **10** (Scheme 2).

Continuation of this strategy to the hexadecamer, **13**, 32-mer, **16**, and 64-mer, **19** was facilitated by the high yields obtained for the deprotection steps, greater than 90% for the desilylation and essentially quantitative for the debenzylation and especially by the efficient coupling step which was 65% even for the coupling of two 32-mers to give the 64-mer, **19**. The structure of the doubly protected 64-mer is shown in Figure 1 with the molecular formula corresponding to a molecular formula of  $\text{C}_{397}\text{H}_{662}\text{O}_{129}\text{Si}$  and a molecular weight of 7522.

Given the precision of the synthetic approach for preparing well-defined caprolactone oligomers and the wide applicability of these materials in fundamental structure/property studies in both biomaterial engineering and polymer physics, it was critical to fully characterize and determine the purity of these materials.

A range of analytical tools were employed to evaluate the purity and molecular weight of the oligomeric/polymeric derivatives including  $^1\text{H}$ ,  $^{13}\text{C}$  NMR, mass spectroscopy (ESI<sup>+</sup>/TOF) combined with MALDI and SEC. As has been found previously with dendrimer syntheses,  $^1\text{H}$  NMR spectroscopy proved to be very diagnostic in following the growth of the polymer chain due to unique resonances for both chain ends and the singular  $\text{CH}_2$  group of the terminal hydroxyl-caprolactone unit. Figure 2 shows the 300 MHz  $^1\text{H}$  NMR spectrum of the doubly protected hexadecamer, **13**, and the resonances for the single benzyl ester chain end can be easily identified at 5.1

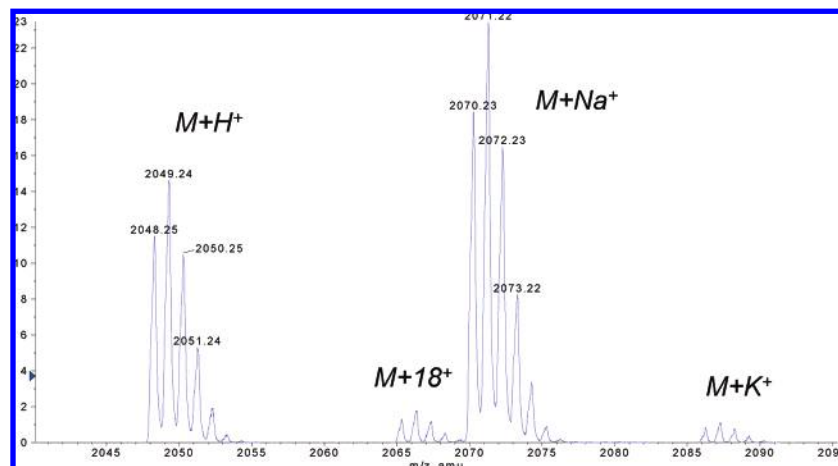


Figure 3. Molecular ions from the ESI-TOF mass spectral analysis of the hexadecamer, **13**.

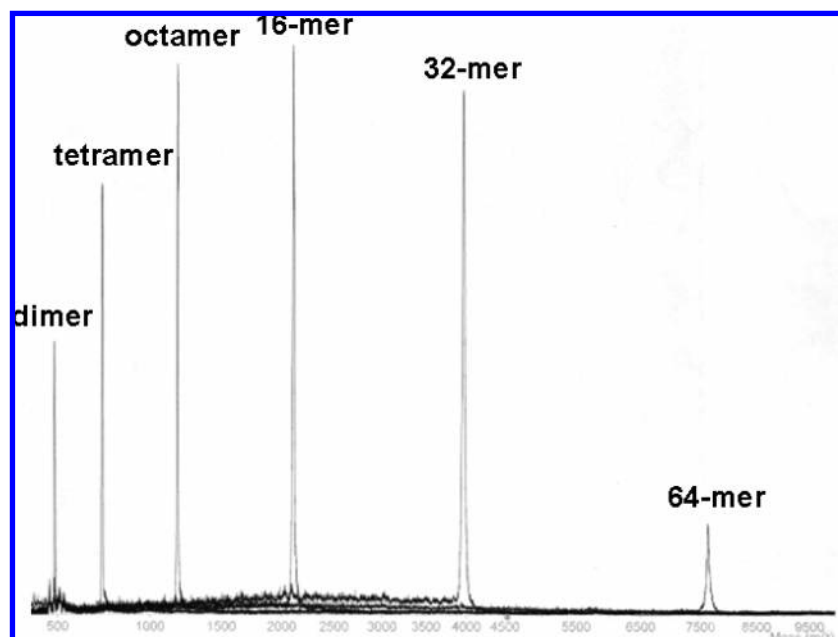


Figure 4. MALDI mass spectra for the caprolactone oligomers from the dimer, **4**, to the 64-mer, **19**.

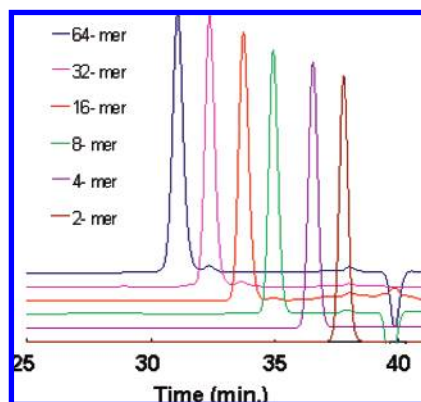
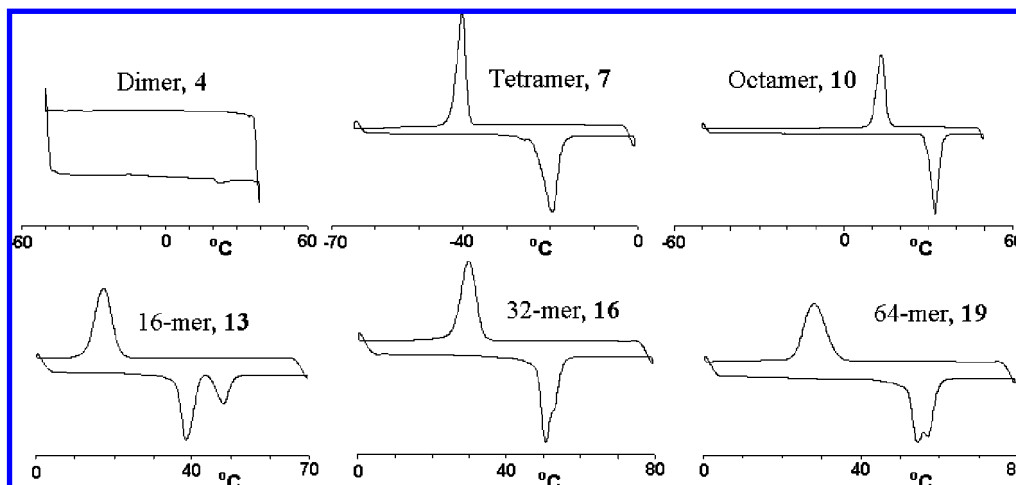


Figure 5. SEC traces for the caprolactone oligomers from the dimer, **4**, to the 64-mer, **19**.

and 7.3 ppm, and the single TBDMS group at the other chain end is similarly clearly distinguishable at 0.0 and 0.85 ppm. Integration of these resonances and comparison with the integration values for the caprolactone backbone allowed the number of repeat units to be determined, which in this case

was shown to be sixteen, as expected from the synthesis. On deprotection, the absence of resonances for the respective chain ends could be easily observed due to the disappearance of peaks above 5.0 and below 1.0 for the backbone, which greatly aided identification of unreacted starting materials during the deprotection reactions. Additionally, the small triplet at 3.65 ppm, due to the unique CH<sub>2</sub> group next to the TBDMSO-group, also functions as a reference peak to monitor the length of the oligo-(caprolactone) backbone and on deprotection to give the HO-group, a shift to 3.60 ppm is observed. Similar trends were observed in the <sup>13</sup>C NMR spectra and further aided structural identification of these materials.

The molecular weights and associated purity for all of the caprolactone oligomers was investigated by both electrospray as well as MALDI mass spectrometry. In all cases, molecular ions for the desired oligomeric species were observed with little or no contamination from failure sequences or chain end impurities. For example, the ESI-TOF spectrum for the doubly protected hexadecamer, **13**, shows only molecular ions corresponding to the hexadecamer as well the corresponding water, Na<sup>+</sup> and K<sup>+</sup> adducts (Figure 3). High-resolution mass spectral



**Figure 6.** DSC traces for the caprolactone oligomers from the dimer, **4**, to the 64-mer, **19**.

analysis of the  $M+Na^+$  ion was also found to correspond with the anticipated molecular formulas. The high degree of purity for all of the oligomers is also represented in the overlay of MALDI mass spectra for the dimer, **4**, to the 64-mer, **19**, showing a prominent molecular ion for all of the oligomers (Figure 4).

To gain a more quantitative understanding of the purity of these materials and the presence of lower molecular weight impurities, size exclusion chromatography analysis of the complete series of oligomers was performed and the results are shown in Figure 5. As expected, the SEC traces are very narrow and monomodal with a complete absence of higher molecular weight impurities for all samples. For the dimer, **4**, to octamer, **10**, derivatives, no low molecular weight impurities are observed; however, a small lower molecular weight peak is observed for the hexadecamer, **13**, 32-mer, **16**, and 64-mer **19**. This lower molecular weight peak corresponded closely with the previous oligomer, that is, 32-mer impurity for the 64-mer and integration showed that the level of impurity was 2% for **13** increasing to 4% for the 64-mer. In combination with the mass and NMR spectroscopy results, it can be concluded that all of the oligomers have a very high level of purity (>95%) and that this predominate structure correlates with that expected from the synthetic strategy.

The availability of molecularly discrete oligomers of poly( $\epsilon$ -caprolactone) allows the systematic study of the influence of molecular weight and chain end structure on the physical properties of this scientifically and commercially important semicrystalline polymer. In comparison, discrete oligomers and polymers of polyethylene have also been prepared and the structure and formation of noninteger and interger folded-chain crystals studied in detail by Ungar.<sup>16</sup> To investigate these unique series of materials, DSC measurements were initially performed on doubly protected derivatives from the dimer, **4**, to the 64-mer, **19**. A composite of DSC traces shown in Figure 6 displays an intriguing progression of crystallinity and melting point

behavior with the dimer, **4**, being totally amorphous. In direct contrast, the tetramer, **7**, and octamer, **10**, show sharp melting transitions at increasing values of  $-20$  and  $32$  °C. Significantly, the behavior for the higher molecular weight oligomers and polymers is dramatically different with the hexadecamer, **13**, having two distinct melting transitions at  $38$  and  $49$  °C, indicating the presence of either two crystallite sizes, a crystal to crystal transition, or two coexisting crystalline structures. This recrystallization of smaller crystallites into larger structures has previously been observed in semicrystalline aliphatic polycarbonates.<sup>17</sup> Doubling the size of the oligomer to the 32-mer, **16**, resulting in merging of these two transitions and a single peak is observed at  $51$  °C with a small shoulder at  $53$  °C, whereas two distinct peaks are again observed for the 64-mer, **19**, with increased melting transitions of  $54$  and  $58$  °C.

The effect of the chain ends on the thermal transitions of the caprolactone oligomers was then investigated by comparing the DSC traces for the 3 possible deprotected derivatives: the acid-terminated 32-mer with a TBDMS protected chain end, **17**, the hydroxy-terminated 32-mer with a benzyl ester protected chain end, **18**, and the doubly deprotected 32-mer with a single hydroxyl and carboxylic chain end, **21**. The latter was obtained in quantitative yield by hydrogenation of **18**. Comparison of these derivatives with the protected 32-mer, **16** (see Figure 6), shows very little difference between all four samples and similar melting/crystallization temperatures, peak shapes in each case. In contrast, comparison of the oligomers with monodisperse poly(caprolactone),  $M_w = 14\,000$ ,  $PDI = 1.1$ , shows significantly broader peaks and altered peak shapes for the commercial PCI sample (Figure 7).

Analysis of the decomposition of the caprolactone oligomers with increasing molecular weight also proved to be very instructive. As shown in Figure 8, there is a well-defined increase in thermal stability from the dimer, **4**, which begins to decompose at  $190$  °C through the tetramer, **7**, ( $275$  °C) and finally the 64-mer, **19**, where decomposition is initiated at  $365$  °C. This dramatic increase in thermal stability is most pro-

(15) (a) Wu, P.; Feldman, A. K.; Nugent, A. K.; Hawker, C. J.; Scheel, A.; Voit, B.; Pyun, J.; Fréchet, J. M. J.; Sharpless, K. B.; Fokin, V. V. *Angew. Chem., Int. Ed.* **2004**, *43*, 3928–3932. (b) Hawker, C. J.; Fréchet, J. M. J. *J. Am. Chem. Soc.* **1990**, *112*, 7638–7647. (c) Ihre, H.; Hult, A.; Soderlind, E. *J. Am. Chem. Soc.* **1996**, *118*, 6388–6395. (d) Percec, V.; Chu, P. W.; Kawasumi, M. *Macromolecules* **1994**, *27*, 4441–4453.

(16) Ungar, G.; Zeng, X.; Brooke, G. M.; Mohammed, S. *Macromolecules* **1998**, *31*, 1875.

(17) (a) Bass, C.; Battesti, P.; Albérola, N. D. *J. Appl. Polym. Sci.* **1994**, *53*, 1745. (b) Kricheldorf, H. R.; Dunsing, R.; Serra, I.; Albert, A. *Makromol. Chem.* **1987**, *188*, 2453. (c) Sarel, S.; Pohoryles, L. A. *J. Am. Chem. Soc.* **1958**, *80*, 4596. (d) Sidoti, G.; Capelli, S.; Meille, S. V.; Alfonso, G. C. *Polymer* **1997**, *39*, 165.

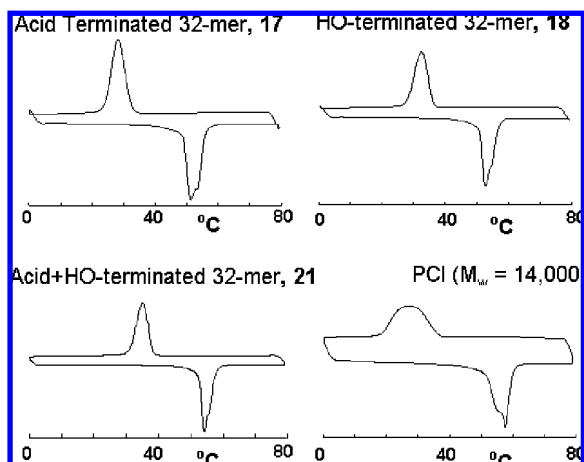


**Figure 7.** Comparison of DSC traces for 32-mers with different chain end substitution, 17, 18, and 21, with commercially available poly(caprolactone).

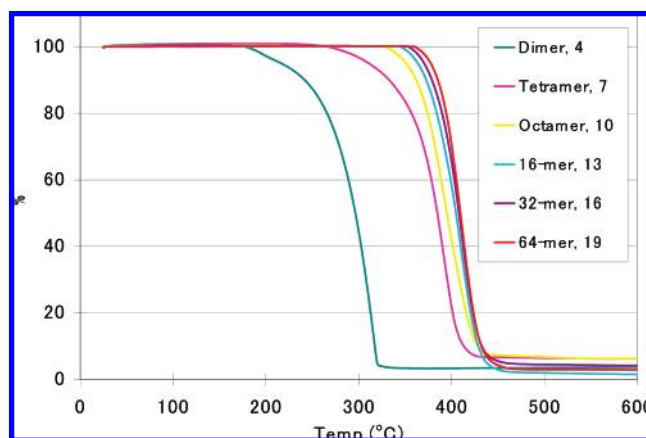


**Figure 8.** Comparison of TGA traces for caprolactone oligomers from the dimer, 4, to the 64-mer, 19. In all cases, the chain ends are TBDMSO and benzyl ester.

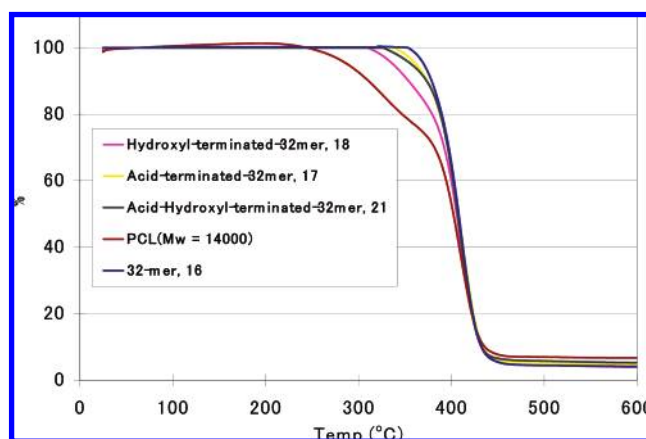


**Figure 9.** Comparison of TGA traces for 4 different chain end functionalized 32-mers, 16, 17, 18, and 21, and comparison with commercially available poly(caprolactone),  $M_w = 14,000$  Da, PDI = 1.1.

nounced on going from 4 to the octamer, 10, with the increase being significantly less for the octamer, 10, to the 64-mer, 19, even though the length of the polymer chain is increased 8-fold. In all cases, the chain ends were the same, a single TBDMS protected hydroxyl group and a single benzyl ester protected carboxylic acid group.

The strong correlation between oligomer length and thermal decomposition profile prompted an examination of the effect

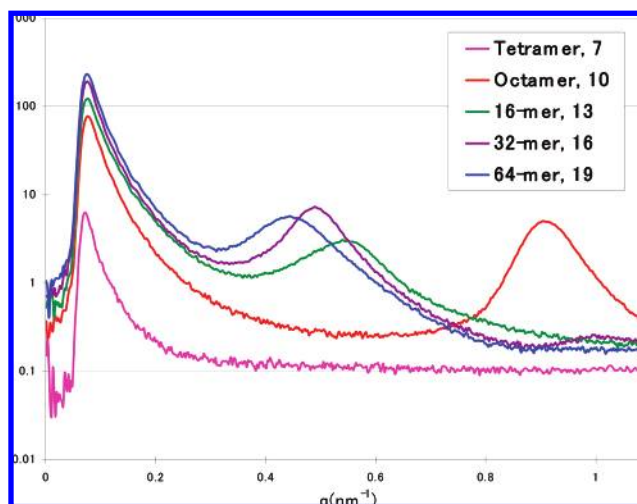


**Figure 10.** SAXS data for oligo(caprolactone) derivatives from the tetramer, 7, to the 64-mer, 19.

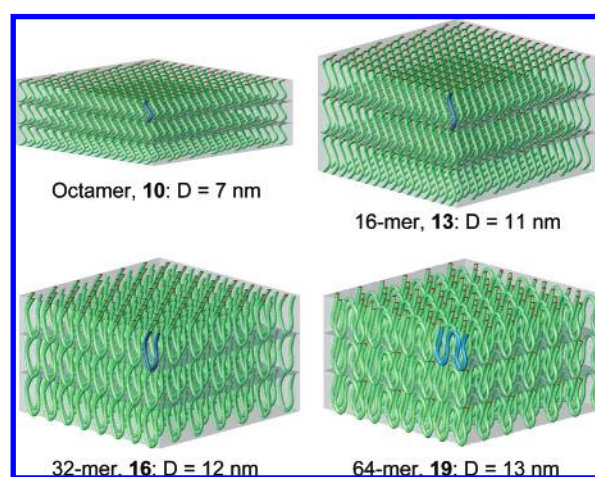


**Figure 11.** Graphical representation of the evolution of crystal structure for caprolactone oligomers from the octamer, 10, to the 64-mer, 19.

of chain end functionality and a direct comparison with commercially available, low polydispersity poly(caprolactone). Of particular note was the observation that all of the 32-mer samples, irrespective of the end groups, were significantly more stable than either commercial poly(caprolactone) ( $M_w = 14,000$ , PDI = 1.1) or a synthetic version of low polydispersity poly(caprolactone) ( $M_w = 15,000$ , PDI = 1.08) that had well-defined ethoxy and carboxylic acid end group. In each case, the onset of decomposition was lower for the polydisperse samples with the commercial sample (poorly defined end groups) being ca. 100 °C and the synthetic derivative ca. 50 °C less stable than the monodisperse derivatives. Interestingly, the 32-mer with the lowest thermal stability was the mono-hydroxy, benzyl ester terminated derivative, 18, followed by both the mono-carboxylic acid, TBDMSO-terminated oligomer, 17, and the doubly deprotected, hydroxyl-carboxylic acid 32-mer, 21 (Figure 9). From these results, it is apparent that the presence of a hydroxyl chain end leads to decreased thermal stability, presumably due to the occurrence of chain backbiting and associated depolymerization. The presence of a terminal carboxylic acid group is also destabilizing but to a decreased degree when compared to a hydroxyl group whereas the polydisperse nature and possible impurities in the commercial PCL dramatically decrease thermal stability.

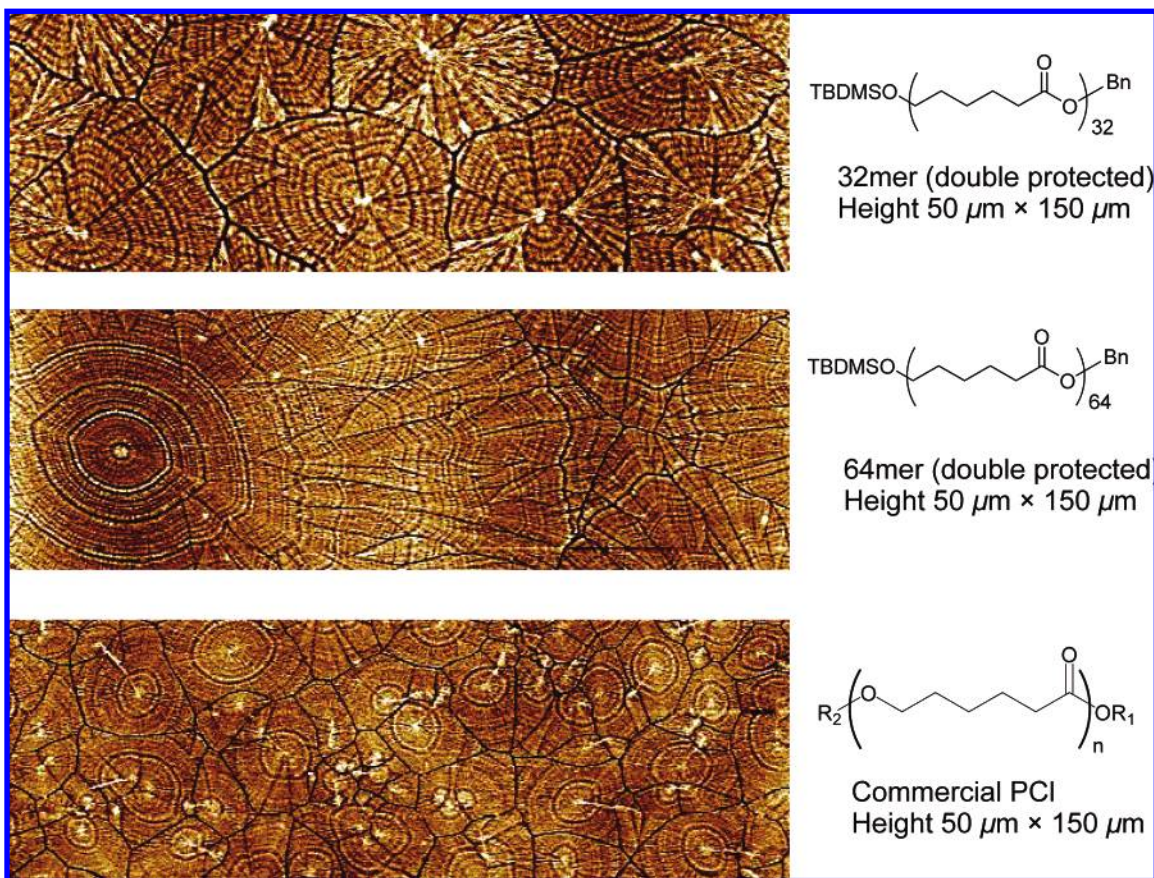


**Figure 12.** Sequence of TM-AFM images for crystallized thin films of the 32-mer, **16**, 64-mer, **19**, and a commercial PCI sample of  $M_w = 14\,000$ , scan size is 50 microns  $\times$  150 microns.

The availability of precisely defined oligomers of a semi-crystalline polymers also represents an unprecedented opportunity to study the effect of molecular size on crystal formation in polyester systems. Preliminary SAXS measurements were therefore conducted at room temperature for the caprolactone derivatives from the tetramer, **7**, to the 64-mer, **19** (Figure 10). As expected, the tetramer did not show any crystalline structure at room temperature, however all other samples displayed a lamellae morphology. For the octamer, **10**, and the 16-mer, **13**, the thickness  $D$  of the lamellae structure (7 and 11 nm, respectively) was very close to the theoretical molecular lengths (7 and 12 nm, respectively), indicating that the chains are fully extended in the lamellae structure.

In direct contrast, the 32-mer, **16**, and 64-mer, **19**, were shown to have lamellae thicknesses significantly smaller than the calculated molecular lengths. SAXS analysis showed a thickness of 12 nm for **16** and 13 nm for **19**, which is approximately 50 and 30% of their respective theoretical extended chain lengths of 23 and 46 nm. This suggests that the 32-mer, **16**, is folded once and the 64-mer, **19**, is folded multiple times. Significantly, the nature of the chain end groups showed no detectable effect on the SAXS profiles for the 16-mer, 32-mer and 64-mer series of derivatives, which suggests that the crystal structure is predominately determined by the length of the oligomer and not the chain end functional groups. As a result, a preliminary, graphical picture can be drawn for the evolution of crystal structure with molecular weight for poly(caprolactone) with increasing lamellae thickness up to the 16-mer resulting in a maximum in crystal thickness and the occurrence of chain

folding at higher chain lengths (Figure 11). A similar crystal thickness was also observed for the low polydispersity poly-(caprolactone) sample with a molecular weight of 14 000, indicating that the lamellae thickness was again approximately 16 repeat units, though the peak was broader. A more detailed study of the structure and morphology of these semicrystalline oligomers is currently under way.

A similar strong dependence of crystal shape on molecular weight and polydispersity of the sample was observed by atomic force microscopy. Analysis of the oligomers showed a systematic increase in crystallite size with monomer length for thin films under both normal spin casting conditions and after identical thermal annealing profiles. As can be seen in Figure 12, the size of the crystallites increases from ca. 30 microns for the 32-mer, **16**, to over 100 microns for the 64-mer, **19**. Interestingly, increasing the molecular weight from 7318 for the 64-mer to a  $M_w$  of 14 000 for the commercial PCI sample gave significantly different results with a multitude of small, ca. 10 micron, crystallites being formed. This study again demonstrates the significant difference in physical properties and behavior between the well-defined oligomers and low polydispersity, commercial PCI materials of comparable molecular weight and a systematic, in-depth examination of the thin film properties of these materials is in progress.

## Conclusions

A synthetic strategy for the preparation of well-defined  $\epsilon$ -caprolactone oligomers up to the 64-mer was developed using an iterative divergent-convergent approach. By the selection of



orthogonal protecting groups, *t*-butyldimethylsilyl ether and benzyl ester, high yields of the oligomers were obtained and the effect of both oligomer length and chain end functionality examined. Characterization of each oligomer by a combination of spectroscopic and chromatographic techniques revealed >95% purity for each oligomer and a direct correlation between oligomer length and thermal properties was observed. Increasing molecular length led to novel semicrystalline behavior being observed for each of the oligomers above the tetramer. A similar relationship between oligomer length and crystal structure was observed by SAXS measurements which showed formation of lamellae crystals that increased in thickness with oligomer length up to the 16-mer, after which the chains undergo folding with a unit length of approximately 16 caprolactone units. The availability of well-defined oligomers of poly( $\epsilon$ -caprolactone)

allows new insight into the fundamental physical and biomaterial properties of this widely studied and commercially important polymer.

**Acknowledgment.** Financial support from the NSF, MRSEC Program DMR-0520415 (MRL-UCSB), Mitsubishi Chemical Center for Advanced Materials (MC-CAM), and Mitsubishi Chemical Group Science and Technology Research Center, Inc. is gratefully acknowledged.

**Supporting Information Available:** Instrumentation and analytical techniques; synthetic procedures for oligomer and intermediates. This material is available free of charge via the Internet at <http://pubs.acs.org>.

JA077149W